

The influence of negative work on optimal flapping flight[†]

Christopher O. Johnston¹, William H. Mason¹ and Cheolheui Han²

¹Department of Aerospace and Ocean Engineering, Virginia Polytechnic Institute and State University, Blacksburg, VA 24060, USA

²Department of Aeronautical and Mechanical Design Engineering, Chungju National University, 50 Daehak-Ro, Choongbuk, 380-702, Korea

(Manuscript Received January 29, 2010; Revised August 30, 2010; Accepted October 11, 2010)

Abstract

This paper examines the influence of negative work on energy required for the flapping wing flight of birds, or other flapping wing animals or vehicles. Because negative energy is typically required by muscles or actuators to produce negative work, it must be accounted for when determining the most efficient flapping configuration. The present work provides a simple theoretical analysis for determining the influence of negative work by introducing a simple actuator/muscle model, which specifies the amount of input energy required to produce negative or positive work. The influence of aerodynamic, structural, and inertial forces are treated in the study. The aerodynamic forces are modeled using unsteady thin airfoil theory, which is appropriate for the relatively high aspect ratio wings of most birds. The influence of springs on a flapping system are discussed, and theoretical approach to determine the spring stiffness required to minimize negative work is presented. The developed analysis is applied to a Pigeon and a Pied Flycatcher. It is found that the flight speed requiring minimum muscle energy is dependent upon the energy cost of negative work.

Keywords: Aerodynamic work; Flapping wing aerodynamics; Thin airfoil theory; Von Karman and Sears approach; Unsteady aerodynamics

1. Introduction

With the help of recent rapid progress on the development of light-weight and small-size actuators, Micro Aerial Vehicles (MAV) that are mimicking insects or birds have been developed or under construction. Birdlike flapping MAVs may have a number of advantages in terms of range or endurance compared to insect mimicking MAVs.

Azuma [1] reviewed the aerodynamics of wing beatings based on the theoretical and experimental data published in the literature. Extensive reviews on flapping foils and their applications to the development of aerial or marine vehicles were also given by Rozhdestvensky and Ryzhov [2] and Ho et al. [3], respectively. Various aspects of fixed and flapping wing aerodynamics for MAV applications are well introduced in Ref. [4].

With the increasing practicality of computational fluid dynamics, the progress has been made on the revealing the secrets of insect or bird flight. However, computational fluid dynamics study using the Navier-Stokes equations requires huge computing time and costs. Based on advanced flow visualization technology with a high-speed camera, a digital particle image velocimetry is used to analyze the flow struc-

ture around the live animals or model robots. The experimental study requires a model that can represent complete geometry and kinematics of live birds, which also results in a large amount of time and costs. Thus, the research on the aerodynamics of bird wings is mostly based on the theoretical or simple numerical results.

Philips et al. [5] used a simple lifting-line approach in their aerodynamic analysis of bird flight. They separated the wake region as two parts: a near wake region traced out most nascently vorticity by the wings, and a far wake region where the vorticity evolves with stretching and dissipation mechanism. Liu [6] compared the flapping-wing and fixed-wing flyers using a scale analysis. He also developed a time-area-averaged momentum stream tube model for analysis of flapping flight [7]. Numerical studies considering the complete geometry and kinematics of live birds are rarely found in the literature. Recently, Liu et al. [8] reported the geometry and kinematics of several avian wings including seagull's. Han [9] numerically implemented the geometry of the seagull wing and its kinematics based on the Liu et al.'s data [8]. He reported that the effect of the combination of flapping, folding, and lead&lag.

The energy required by the muscles of birds is in many ways analogous to the actuators of an artificial flapping-wing flight vehicle. One important similarity is that in both cases the energy input required by a muscle or actuator to produce positive (where a force opposes the motion) and negative work (where a force acts in the same direction as the motion) is different.

[†]This paper was recommended for publication in revised form by Associate Editor Haecheon Choi

*Corresponding author. Tel.: +82 43 841 5379, Fax.: +82 43 841 5370

E-mail address: chhan@cjnu.ac.kr

© KSME & Springer 2010

The energy required by actuators or muscles to drive the flapping motion of a wing was treated in the previous literatures for the analysis of animal flight or swimming [10-13] as well as the design of a flapping-wing flight vehicle [14-17]. Brooks et al. [18] applied a series arrangement for a flapping pterosaur model and showed that this resulted in a large reduction in the actuator current required for flapping. Bennett et al. [19] studied the muscles in the tails of whales and found that the muscles were in series with elastic tissue. They attempted to show that this configuration minimized the negative work required by the muscles, but found that it actually did not. Blickhan and Cheng [20] revisited the study of Bennett et al. [19] and found that the elastic tissues did in fact reduce the amount of negative work required by the muscles. They used an unsteady vortex lattice method to model the aerodynamics and showed that Bennett's simplified quasi-steady aerodynamic model was insufficient. Pennycuick [21] studied the elastic properties of feather shafts in birds and showed that they were capable of acting as an efficient spring. It was not made clear whether this was a parallel or series arrangement. Weis-Fogh [22] studied the elastic properties of insect cuticles, which acted as springs in the hinges of insect wings. Because the spring was at the hinge, it was a parallel configuration. Weis-Fogh [23] later concluded from an energy analysis, which considered only the positive work, that these elastic mechanisms must be present for insect flight to be possible. In another similar study, Weis-Fogh [11] discussed the possible benefits of elastic elements in hummingbirds, but mentioned that no such system was found upon dissecting a hummingbird. Furthermore, it was mentioned that no elastic system has been found by any researcher in any bird. Of course, as was mentioned previously, Pennycuick [21] later found a type of elastic mechanism, although the effectiveness of this mechanism was not confirmed.

Most of previous researches have focused on single discipline such as aerodynamics or structural dynamics. However, the development of the feasible flapping MAVs with outstanding flight performance requires more than the single disciplines alone. It needs the integration of several disciplines including at least aerodynamics, structure, and inertia models. However, an integrated research considering aerodynamics, structure, and inertia models has not much shown in the published literature. Computational methods that can solve the problems that include aerodynamics, structure, and inertia models is still under development and hard to use for the practical applications. Due to the unsteadiness of the problem, simultaneously measuring the small aerodynamic forces hidden in the large inertial forces are not easy. Thus, in this paper, the influence of negative work on the optimal flapping configuration of a flapping wing flight vehicle is evaluated by developing a simplified actuator/muscle model. The integrated aerodynamic, structural, and inertia models are derived for the optimal spring stiffness for minimum negative work. Present analysis is applied to a three-dimensional flapping wing vehicle.

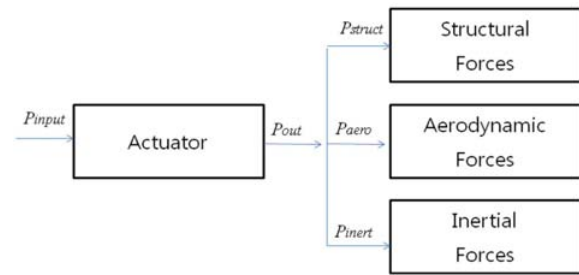


Fig. 1. The distribution of the provided actuator power for a general configuration.

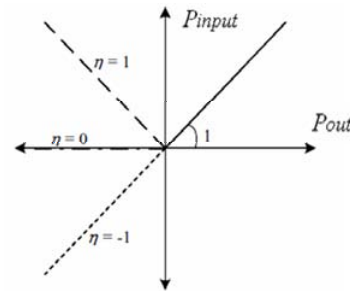


Fig. 2. The relationship between P_{out} , the required rate of actuator work, and P_{input} , the rate of actuator energy, for the proposed general actuator model.

2. Theory

2.1 Actuator/Muscle energy model

Fig. 1 shows one way of allocating the total required actuator power (P_{out}) for a general flapping wing. To obtain the quantity P_{input} , the knowledge of the actuator energetics and actuator placement is required. For the current study, which is intended to investigate the fundamentals of the actuator energy required for flapping wing flight, a general model of the actuator energetics is proposed. For the present model, if $P_{out} \geq 0$, meaning positive work is required, then $P_{input} = P_{out}$, while if $P_{out} < 0$, meaning negative work is required, then $P_{input} = \eta|P_{out}|$. In these relationships, η is a constant ranging from -1 to 1 depending on the actuator. A separate efficiency could be defined for positive values of P_{out} (so that 100% actuator efficiency is not assumed), although this implies just multiplying W_{input} by a constant (since η will change accordingly).

Fig. 2 illustrates the above relationships for three key values of η . For $\eta = 1$, the actuator requires the same power input to produce negative values of P_{out} as it does to produce positive values. Recall that positive P_{out} values indicate that the actuator motion is resisted by the external forces while negative values indicate that the external forces act in the direction of actuator motion. For $\eta = 0$, the actuator requires no power input and allows no power to be extracted while producing negative values of P_{out} . This case is the most consistent with feedback controlled pneumatic [24] and hydraulic actuators [25], which require only the controlled release of pressurized fluid to produce negative power. The neglecting of negative

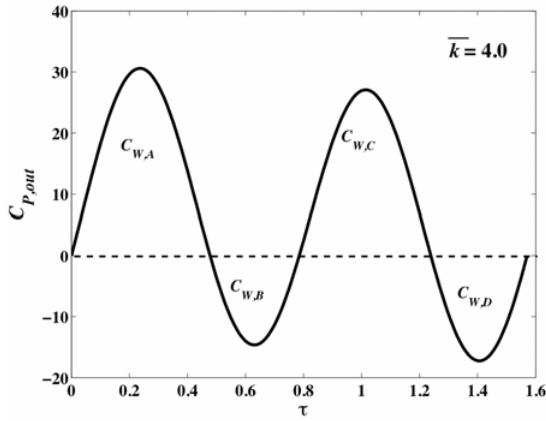


Fig. 3. Example of terms in Eq. (1) for a single flapping cycle.

work values has also been considered for the energy-cost analysis of insect flight [23] and human muscles [26]. The $\eta = -1$ case allows the actuator to store the incoming energy associated with negative values of P_{out} to be used later to produce positive P_{out} values with 100% conversion efficiency. This value of η allows W_{input} to be negative and zero for certain cases. Negative values of η are possible for piezo-electric actuators due to their electro-magnetic coupling [27].

Throughout the present study, the power and work will be written in terms of the non-dimensional power coefficient, $C_p = P/qUc$, and work coefficient, $C_w = W/qc^2$, where q is the dynamic pressure, W is the work, U is the free stream velocity, and c is the airfoil chord length. Also used throughout this study are the reduced frequency, $\bar{k} = \omega c/U$, and nondimensional time, $\tau = Ut/c$, where ω is the frequency of the flapping motion.

From the general actuator model of Fig. 2, the equation for the total required actuator energy input can be written as

$$C_{W,input} = C_{W,out+} + \eta C_{W,out-} \tag{1}$$

where $C_{W,out+}$ and $C_{W,out-}$ are the absolute values of the positive and negative components of $C_{W,out}$. These components are shown for a single flapping cycle in Fig. 3, where in this case $C_{W,out+}$ is equal to the sum of $C_{W,A}$ and $C_{W,C}$ while $C_{W,out-}$ is equal to the sum of $C_{W,B}$ and $C_{W,D}$. The average value of $C_{P,input}$ is defined as $\bar{C}_{P,input} = C_{W,input} \bar{k} / 2\pi$, which will be used for efficiency calculations.

2.2 Flapping wing energetics

The present aerodynamic model is based on two dimensional unsteady thin airfoil theory. In this model, pure flapping motion is represented by a heaving motion, meaning the airfoil section is moving vertically up and down. The airfoil motion is represented by the parameter β , which is written as $\beta = \beta_0 + \bar{\beta} \cos(\bar{k}\tau)$, where β_0 is the steady angle-of-attack and $\bar{\beta}$ is the amplitude of the oscillating motion.

From thin airfoil theory [28,29], the aerodynamic power coefficient, $C_{P,aero}$, is written as

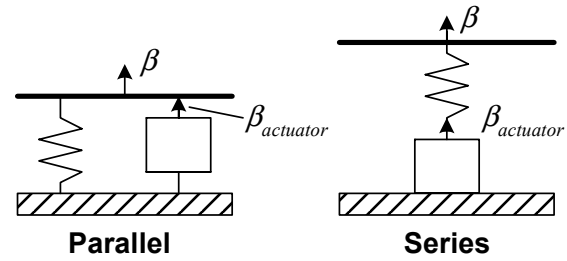


Fig. 4. Illustration of a spring and actuator in parallel and in series.

$$C_{P,aero}(\tau) = \bar{\beta}^2 \left[\Phi_1(\bar{k}) \cos(\bar{k}\tau) + \Phi_2(\bar{k}) \sin(\bar{k}\tau) \right] \sin(\bar{k}\tau) + \bar{\beta}_0 \bar{\beta} \Phi_3(\bar{k}) \sin(\bar{k}\tau) \tag{2}$$

where the Φ terms are defined as $\Phi_1(\bar{k}, \theta) = 2\pi\bar{k}^2(\bar{k}/4 + G)$, $\Phi_2(\bar{k}, \theta) = 2\pi\bar{k}^2 F$, $\Phi_3(\theta) = 2\pi\bar{k}$. The F and G functions in these equations are the real and imaginary parts of the well known Theodorsen function [30]. The average value of $C_{P,aero}$ over one cycle is written as $\bar{C}_{P,aero} = \bar{\beta}^2 \Phi_2(\bar{k}) / 2$. Similarly, the average drag coefficient over one cycle is written as $\bar{C}_d = -\pi\bar{k}^2 \bar{\beta}^2 (F^2 + G^2)$. Combining these two equations, the aerodynamic efficiency is written as $\kappa_{aero} = -\bar{C}_d / \bar{C}_{P,aero} = -(F^2 + G^2) / F$, while the actuator efficiency is written as $\kappa_{input} = -\bar{C}_d / \bar{C}_{P,input}$, which requires the evaluation of total actuator input energy, $\bar{C}_{P,input}$.

To determine the total actuator input energy ($\bar{C}_{P,input}$), the structural and inertial power components shown in Fig. 1 must also be known. The power to overcome the inertial forces will be written as

$$C_{P,inert}(\tau) = \bar{\beta}^2 K_I \bar{k}^3 \cos(\bar{k}\tau) \sin(\bar{k}\tau) \tag{3}$$

where $K_I = m_a / \rho c^2$ and m_a is the mass per-unit-length of the airfoil in the spanwise direction. The power required to overcome the structural forces will be simplified as the power required to overcome a spring connected to the flapping device. There are two different arrangements possible for a single actuator and spring: parallel and series. These are shown in Fig. 4, where $\beta_{actuator}$ is the actuator output displacement and β is the resulting airfoil displacement. For the parallel arrangement, $\beta_{actuator}$ and β are the same while for the series arrangement they are added together. Conversely, for the series arrangement, the force acting at $\beta_{actuator}$ and β is the same while for the parallel arrangement they are added together.

For the present analysis, a parallel spring arrangement will be considered. A similar discussion for the series arrangement is presented by Blickhan and Cheng [20]. For a given reduced frequency, the parallel and series arrangements may be designed to give the same optimal performance. The difference between the two comes in their off-design operation. Generally, the series arrangement is significantly better in off-design conditions. For the parallel arrangement, the required power can be written as

$$C_{P,spring}(\tau) = -K_S \left[\bar{\beta} \cos(\bar{k}\tau) - \bar{\beta}_s \right] \bar{\beta} \bar{k} \sin(\bar{k}\tau) \quad (4)$$

where $\bar{\beta}_s$ is the value of β at which the spring produces no force and K_S is nondimensional spring stiffness per-unit length, which is defined as $K_S = X/q$, where X is the dimensional spring stiffness per-unit length (N/m²) and q is the dynamic pressure.

2.3 Influence of springs on optimal flapping

Combining Eqs. (2), (3), and (4), the total output power required by the actuator to maintain the prescribed flapping motion is written as

$$C_{P,out}(\tau) = A/2 - A \cos(2\bar{k}\tau)/2 + B \sin(2\bar{k}\tau)/2 + C \sin(\bar{k}\tau) \quad (5)$$

where $A = \bar{\beta}^2 \Phi_2$, $B = \bar{\beta}^2 (\Phi_1 + K_I \bar{k}^3 - K_S \bar{k})$, and $C = (\bar{\beta}_0 \Phi_3 + K_S \bar{\beta}_s \bar{k}) \bar{\beta}$. The average value of $C_{P,out}$ is equal to $A/2$, which is the same as $\bar{C}_{P,aero}$, meaning the spring and inertia do not contribute. Eq. (5) shows that $C_{P,out}$ will be positive for every value of τ if B and C are zero and Φ_2 is positive. From Eq. (2), it is seen that Φ_2 is always positive (since F is always positive). If K_S and $\bar{\beta}_s$ are free design variables, then from Eq. (5) they can be chosen to make B and C equal to zero. This leads to the following:

$$K_{S,opt} = \Phi_1 / \bar{k} + K_I \bar{k}^2 \quad (6)$$

$$\bar{\beta}_{S,opt} = -\frac{\bar{\beta}_0 \Phi_3}{\Phi_1 + K_I \bar{k}^3}.$$

Because $K_{S,opt}$ is a nondimensional coefficient, it makes things more clear if X_{opt} is written instead, which results in

$$X_{opt} = \rho (\Phi_1 U^3 / (\omega c) + K_I (\omega c)^2) / 2. \quad (7)$$

For a given design condition, which is defined by ω and U separately (i.e. not just \bar{k}), X_{opt} and $\bar{\beta}_{S,opt}$ may be chosen from Eqs. (6) and (7), therefore resulting in Eq. (5) reducing to $C_{P,out}(\tau) = A/2 - A \cos(2\bar{k}\tau)/2$. Assuming X_{opt} and $\bar{\beta}_{S,opt}$ cannot be varied during flight, it is important to know what range of ω and U values that the spring system remains beneficial compared to having no spring. A simplified case of practical significance considers the range of U values for a fixed ω and a $\bar{\beta}_s$ that is always optimal, or $\bar{\beta}_0$ and $\bar{\beta}_s$ may be considered zero (meaning C is always zero). From Eq. (5), the value of B for the case of no spring is written as: $B_0 = \bar{\beta}^2 (\Phi_1(\omega, U) + K_I (\omega c / U)^3)$. At the design value of U (U_{des}), the design value of X (X_{des}) is obtained from Eq. (7) and the corresponding B is equal to zero. At an off-design value of U defined as $U_{off} = U_{des} + \Delta U$, which corresponds to the following value of B :

$$B_{off} = \bar{\beta}^2 \left(\Phi_1(\omega, U_{des} + \Delta U) + K_I \left(\frac{\omega c}{U_{des} + \Delta U} \right)^3 - \frac{2X_{des}\omega}{\rho(U_{des} + \Delta U)^2} \right) \quad (8)$$

For the spring to be beneficial, the inequality $B_0(U_{des} + \Delta U) > B_{off}(U_{des} + \Delta U)$ must be satisfied, which leads to the following equation:

$$0 < \frac{2X_{des}\omega}{\rho(U_{des} + \Delta U)^2} < \Phi_1(\omega, U_{des} + \Delta U) + K_I \left(\frac{\omega c}{U_{des} + \Delta U} \right)^3. \quad (9)$$

The lower limit indicates that ΔU may become as large (positive) as desired and the spring will remain beneficial. To study the upper limit of Eq. (9) (small ΔU or large \bar{k}), it is necessary to substitute Φ_1 from Eq. (2) into Eq. (9), which results in the following:

$$0 < \frac{2X_{des}\omega}{\rho(U_{des} + \Delta U)^2} < 2\pi \left(\frac{\omega c}{U_{des} + \Delta U} \right)^2 F + K_I \left(\frac{\omega c}{U_{des} + \Delta U} \right)^3 \quad (10)$$

where F is a function of ω and U . Considering the large \bar{k} case, F may be approximated in terms of \bar{k} as $F = 0.5(1 + 1/2\bar{k}^2 + O(\bar{k}^{-4}))$ [31]. Substituting this into Eq. (10) and considering the right inequality, the following equation is obtained after some algebra, which may be solved for the lower (negative) limit of ΔU :

$$\pi(U_{des} + \Delta U)^3 / 2 + (\pi(\omega c)^2 - 2X_{des}\omega / \rho)(U_{des} + \Delta U) + (\omega c)^3 K_I = 0. \quad (11)$$

In summary, ΔU may be as large and positive as desired for the spring designed for U_{des} to be beneficial over the no spring case, but beyond the negative ΔU found from Eq. (11), the system requires more energy than if there was no spring.

2.4 Flapping wing flight performance

This section will investigate the actuator input energy required by a full flapping wing vehicle using the theoretical developments of the previous sections. There has been a significant amount of past research to determine the energy required for flapping flight (a review is presented by Shyy et al. [32]), although nearly all of it has been concerned with determining the output energy required by actuators or muscles instead of the input energy required. Because the role of negative work could be large, the required output energy required by actuators does not provide sufficient guidance towards an energy efficient flapping device.

Fig. 5 shows the front view of a half-span, where the dark line is the wing surface and s is the wing half-span. The ampli-

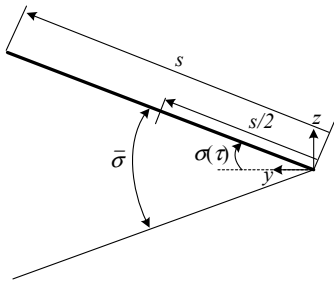


Fig. 5. Front view of a half-span of the flapping wing.

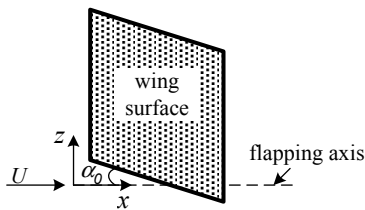


Fig. 6. Side view of a half-span of the flapping wing.

tude of the total flapping motion is defined by $\bar{\sigma}$ and the instantaneous flap angle measured from the y -axis is defined as $\sigma(\tau) = \bar{\sigma} \cos(\bar{k}\tau)/2$. We will treat the airfoil section at the span location $s/2$ as the representative section for the half span. To apply the heaving airfoil equations to this section, the maximum arc-length measured from the y -axis is β , which is written as $\beta(\tau) = s\bar{\sigma} \cos(\bar{k}\tau)/4c$, which implies that $\bar{\beta} = s\bar{\sigma}/4c$.

Fig. 6 shows the side view of a half-span, which shows that the flapping axis is assumed to remain parallel to the free-stream velocity.

The steady-state lift for the configuration is assumed to be produced by the angle of attack (α_0) of the wings relative to the flapping axis. The difference between the flapping axis being at an angle of attack and the wings relative to the flapping axis being at an angle of attack is not large if $\bar{\sigma}$ is less than 45 degrees. The normal force coefficient of the entire wing is written as

$$C_N = 2\pi(\alpha_0 - w_0) + \text{unsteady terms} \tag{12}$$

where the three-dimensional downwash correction used by DeLaurier [33] is defined as $w_0 = 2\alpha_0/(2 + AR)$, and AR is the wing aspect ratio. To obtain the average lift coefficient for one cycle of oscillation, the following equation is used

$$\bar{C}_L = \frac{\bar{k}}{2\pi} \int_0^{2\pi/\bar{k}} C_N \cos(\sigma) d\tau \tag{13}$$

which from Eq. (12) and the above definition of σ results in

$$\bar{C}_L = 2\pi\alpha_0 J_0(\bar{\sigma}/2) \left(1 - \frac{2}{2 + AR}\right) \tag{14}$$

where J_0 is a zeroth order Bessel function of the first kind.

For steady level flight, the average lift must balance the weight of the aircraft, which is expressed in the following equation

$$qS\bar{C}_L - mg = 0 \tag{15}$$

where S is the wing area, m is the aircraft mass, and g is gravity. Also, for steady flight the thrust must equal the drag, which is expressed as

$$\frac{(qS\bar{C}_L)^2}{4e\pi q s^2} + qS(C_{d,pro} + C_{d,par}) + qS\bar{C}_d = 0 \tag{16}$$

where the first term is the induced drag, the second term is the profile drag, the third term is the parasite drag, and the fourth term is the unsteady drag (or thrust) component presented in the discussion of Eq. (2). The profile and parasite drag terms are discussed by Pennycuik [10], Tucker [34] and Rayner [12,13] in the context of bird flight. Although the present analysis is not specific to bird flight, the value for $C_{d,pro}$ given by Rayner and the expression for $C_{d,par}$ given by Tucker [34] will be used:

$$C_{d,pro} = 0.02$$

$$C_{d,par} = 3.34 \times 10^{-3} m^{2/3} / S \tag{17}$$

where m is in kg and S is in m^2 . For a given aircraft mass (m), wing area (S), half-span (s), and dynamic pressure (q), the thrust due to flapping ($-\bar{C}_d$) must equal the combination of induced, parasite, and profile drag. From Eq. (16), this results in the following required value of \bar{C}_d

$$\bar{C}_{d,req} = -\frac{(mg)^2}{4Se\pi q^2 s^2} - (C_{d,pro} + C_{d,par}) \tag{18}$$

From the equation presented in the discussion of Eq. (2), the average drag due to flapping produced by a given $\bar{\sigma}$ and \bar{k} is written as

$$\bar{C}_d = -\pi\bar{k}^2 (s\bar{\sigma}/4c)^2 [F^2 + G^2], \tag{19}$$

which must be negative to indicate thrust. The components of the Theodorsen function, F and G , in Eq. (19) are incorrect for finite aspect ratio wings. Jones [35] presented aspect ratio corrections and DeLaurier [33] presented a simplified form of Jones's equations, which are written as follows:

$$F(\bar{k}) = \frac{AR}{(2 + AR)} \left(1 - \frac{C_1 \bar{k}^2}{4(\bar{k}^2/4 + C_2^2)}\right)$$

$$G(\bar{k}) = -\frac{AR}{(2 + AR)} \left(\frac{C_1 C_2 \bar{k}}{2(\bar{k}^2/4 + C_2^2)}\right) \tag{20}$$

where $C_1 = 0.5AR/(2.32 + AR)$ and $C_2 = 0.181 + 0.772/AR$.

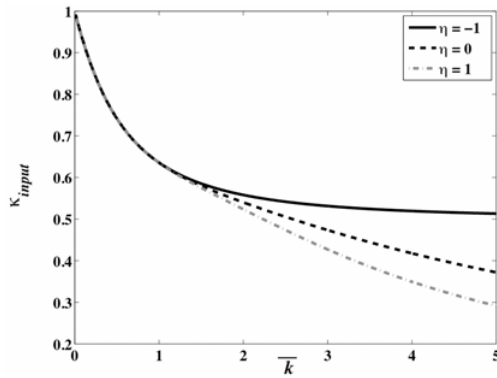


Fig. 7. The efficiency of propulsion for a heaving airfoil (no inertia or spring components).

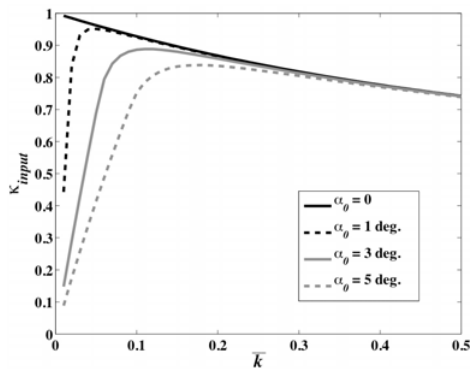


Fig. 8. The efficiency (no inertia or spring components) for different α_0 values.

Equating Eq. (19) with Eq. (18) and assuming U and ω are given, the required flapping amplitude is found to equal

$$\bar{\sigma} = \frac{4c}{s} \sqrt{\frac{\frac{(mg)^2}{e\pi q^2 S b^2} + 0.02 + 3.34 \times 10^{-3} m^{2/3} / S}{\pi \bar{k}^2 (F^2 + G^2)}}. \quad (21)$$

Substituting this into the equation for $\bar{C}_{P,aero}$ presented with Eq. (2), the average aerodynamic power for one cycle is written as

$$\bar{C}_{P,aero} = \left(\frac{(mg)^2}{4Se\pi q^2 S^2} + 0.02 + 3.34 \times 10^{-3} m^{2/3} / S \right) \frac{F}{F^2 + G^2}. \quad (22)$$

Note that this equation is just the average required thrust divided by the aerodynamic efficiency: $-\bar{C}_{d,req} / \kappa_{aero}$. Also, this equation is independent of the spanwise location of the chosen representative airfoil section.

With $\bar{\sigma}$ known from Eq. (21), the required angle of attack (α_0) is determined by combining Eqs. (14) and (15), which results in

$$\alpha_0 = mg \left[2\pi q S J_0(\bar{\sigma}/2) \left(1 - \frac{2}{2 + AR} \right) \right]^{-1}. \quad (23)$$

This is the last term required to calculate $\bar{C}_{P,out}$ from Eq. (5) for a given aircraft configuration (AR, S, s, m, m_a), flight speed (U), and flapping frequency (ω). The average actuator input power ($\bar{C}_{P,input}$) is determined numerically by separating the positive and negative components of $\bar{C}_{P,out}$, as shown in Fig. 3. Note that $\bar{C}_{P,input}$ is dependent upon α_0 , which represents the steady lift component, whereas $\bar{C}_{P,out}$ is not. In the case of swimming flapping wing propulsion, the value for m in the above analysis is set to zero. Also, the parasite and profile drag coefficients in Eq. (17) must be changed to account for the fluid being water instead of air.

3. Results and discussion

3.1 Efficiency of heaving motion with no spring or inertial forces

Results for the total efficiency (κ_{input}) of a heaving airfoil with no spring or inertia forces are shown in Figs. 7 and 8. In Fig. 7, the effect of negative work is seen to greatly reduce the efficiency for large values of reduced frequency. The cases shown in this figure have no constant lift component ($\bar{\beta}_0 = 0$).

As stated earlier in Eq. 2, the $\eta = -1$ case allows the actuator to store the incoming energy associated with negative values of P_{out} to be used later to produce positive P_{out} values with 100% conversion efficiency. However, in the current simulation, the airfoil has no spring forces. Thus, the energy conversion is incomplete, which results in the augmentation of the required energy. As the frequency increases, the incomplete energy conversion or lack of spring deteriorates the efficiency more significantly.

Fig. 8 shows the effect of $\bar{\beta}_0$ being nonzero, where in these cases $\bar{\beta}_0$ represents a constant angle of attack (α_0). For small values of reduced frequency, the difference in the efficiency with $\eta = 1$ is seen to be large. For large values of reduced frequency, the different values of α_0 converge to the zero lift case shown in Fig. 8.

3.2 Flapping wing flight performance analysis

The theory developed for the flapping wing is applied to two flapping wing cases: a Pigeon and a Pied Flycatcher, which have been studied previously by Pennycuik [10], Rayner [13], and Philips et al. [5]. Philips et al. [5] presents a comparison of the three studies. These past studies only calculated the average aerodynamic power ($\bar{C}_{P,aero}$), therefore ignoring the difference in the energy cost of positive and negative muscular work. The present analysis will calculate the average input power ($\bar{C}_{P,input}$) to the flapping actuators. From Weis-Fogh's [11] statement that there are no elastic mechanisms in the wing of a bird, no spring will be present in our analysis. The inertia will also be ignored, which has been assumed negligible in past studies. To be consistent with the comparison presented by Philips et al. [5], the results are presented in terms of the dimensional average power, which for the three-dimensional wing is defined as $\bar{P}_{input} = qUS\bar{C}_{P,input}$.

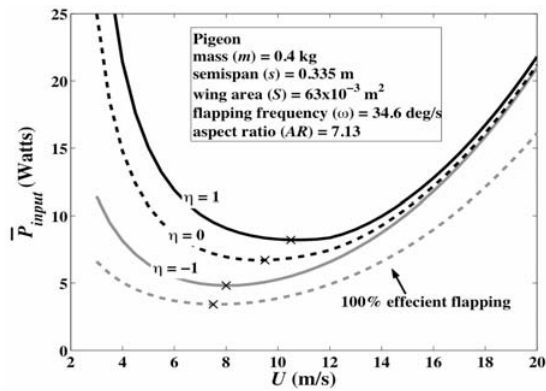


Fig. 9. Average actuator input power versus flight speed for a Pigeon.

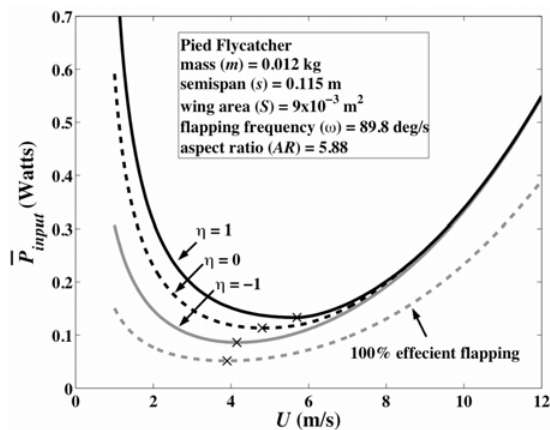


Fig. 10. Average actuator input power versus flight speed for a Pied Flycatcher.

Figs. 9 and 10 present the defining parameters for each bird as well as the power curves resulting from the present method. Recall that for the $\eta = -1$ case, $\bar{C}_{P,input} = \bar{C}_{P,aero}$, which should therefore be in closest agreement with the curves presented by Philips et al. [5]. This is the case, and the present method with $\eta = -1$ predicts a minimum power of nearly equal magnitude at about the same flight speed as the past studies. For the η equal to zero and one cases, the required power is noticeably increased at low flight speeds. This means that there is a significant amount of negative power required during the flapping cycle. An important consequence of this is seen to be the change in the minimum power flight speed, which is marked by an X in both figures. For both birds, the minimum power flight speed increases as η increases. The reason for the large amount of negative power at low flight speeds, which correspond to large values of α_0 , is apparent from Fig. 8. If a spring was added to this system with a K_S and $\bar{\beta}_S$ determined from Eq. (6), the η equal to zero and one curves would reduce to the $\eta = -1$ curve. Thus, a significant reduction in the required power would be obtained. Note that adding an inertia term to this case would increase the amount of negative power; meaning a spring would be even more beneficial. The importance of springs in flapping wing flight is not often mentioned in the literature.

The curve labeled “100% flapping efficiency” in Figs. 9 and 10 represents the required thrust from Eq. (18) multiplied by the velocity. This power would be required from the engine of a fixed wing aircraft of the same size and mass. Thus, there is an apparent penalty for flapping wing propulsion. It could be argued that a fixed wing aircraft would require a larger mass to account for an engine, and therefore this penalty would not be present. Woods et al. [36] compared the power requirements of flapping wings, rotary wings, and fixed wings for micro air vehicles. For a 50 g vehicle, flapping wings were shown to require less power in a range of flight velocities between 3 and 10 m/s. Spedding and Lissaman [37] also discussed the power requirements for small flapping or fixed wing vehicles. They found that flapping and rotary wings have similar power requirements. Thus, it can be decided that the flapping MAV requires less power than the fixed-wing MAV at the low-speed range less than 10 m/s.

4. Conclusions

The theory for determining the influence of aerodynamic, structural, and inertial forces on the negative work for flapping motions of bird is derived by introducing a simple actuator/muscle model. The aerodynamic forces are modeled using unsteady thin airfoil theory. The influence of springs on a flapping system are discussed, and theoretical approach to determine the spring stiffness required to minimize negative work is presented.

From the derived theory, it is found that the negative work does not affect the power requirement when the spring and inertial forces are relatively smaller than the aerodynamic load. It is also found that, in case of the airfoil with no spring forces, the incomplete energy conversion increases the total required energy at high frequency region.

The developed analysis is applied to a Pigeon and a Pied Flycatcher. It is found that the flapping MAV requires less power than the fixed-wing MAV at the low-speed range less than 10 m/s. The flight speed requiring minimum muscle energy is dependent upon the energy cost of negative work.

It is believed that present results can be used for the validation of the numerical methods and the derived theory can also be applied to the design of the flapping wing MAV.

Acknowledgment

The corresponding author's research is partially supported by Basic Science Research Program through the National Research Foundation of Korea (NRF) funded by the Ministry of Education, Science and Technology (KRF-2009-0076384) and by a grant from the Academic Research Program of Chungju National University in 2010.

References

- [1] A. Azuma, *The Biokinetics of Flying and Swimming*, AIAA

- Education Series, 2nd Edition, AIAA, Inc., Reston, Virginia (2006).
- [2] K. V. Rozhdestvensky and V. A. Ryzhov, Aerohydrodynamics of flapping-wing propulsors, *Progress in Aerospace Sciences*, Vol. 39, pp. 585-633 (2003).
- [3] S. Nassef, H. Ho, N. Pornsinsirak, Y-C. Tai and C-M. Ho, Unsteady aerodynamics and flow control for flapping wing flyers, *Progress in Aerospace Sciences*, 39 (2003) 635-681.
- [4] T. J. Muller et al., Fixed and flapping wing aerodynamics for micro air vehicle applications, *Progress in Astronautics and Aeronautics*, Vol. 195, Edited by T. J. Muller, AIAA, Inc. Reston, Virginia (2001).
- [5] P. J. Phillips, R. A. East and N. H. Pratt, An Unsteady Lifting Line Theory of Flapping Wings with Application to the Forward Flight of Birds," *Journal of Fluid Mechanics*, 112 (1981) 97-125.
- [6] T. Liu, Comparative scaling of flapping- and fixed-wing flyers, *AIAA Journal*, 44 (1) January 2006.
- [7] T. Liu, Time-area-averaged momentum stream tube model for flapping flight, *Journal of Aircraft*, 44 (2) March–April 2007.
- [8] T. Liu, K. Kuykendoll, R. Rhew and S. Jones, Avian wing geometry and kinematics, *AIAA Journal*, 44 (5) (2006) 954-963.
- [9] C. Han, Unsteady aerodynamics of seagull wings in level flight, *Journal of Bionic Engineering* (2009).
- [10] C. J. Pennycuik, Power requirements for horizontal flight in the pigeon *Columba livia*, *Journal of Experimental Biology*, 49 (1968) 527-555.
- [11] T. Weis-Fogh, Energetics of hovering flight in hummingbirds and in drosophila, *Journal of Experimental Biology*, 56 (1972) 79-104.
- [12] J. M. V. Rayner, A vortex theory of animal flight: Part 2. The Forward Flight of Birds," *Journal of Fluid Mechanics*, 91 (1979a) 731-763.
- [13] J. M. V. Rayner, A new approach to animal flight mechanics, *Journal of Experimental Biology*, 80 (1979b) 17-54.
- [14] X. Deng, *Flapping Flight for Biomimetic Robotic Insects: System Modeling and Flight Control in Hover*. Ph. D. Dissertation, University of California, Berkeley Department of Mechanical engineering, Electrical Engineering, Aug 2005.
- [15] S. H. McIntosh, *Design and Analysis of a Mechanism Creating Biaxial Wing Rotation for Applications in Flapping-wing Air Vehicles*, Ph. D. Dissertation, University of Delaware, Department of Mechanical Engineering, Jun 2006.
- [16] L. Schenato, *Analysis and Control of Flapping Flight: From Biological to Robotic Insects*, Ph. D. Dissertation, University of California, Berkeley, Department of Electrical Engineering, Aug 2004.
- [17] J. Yan, *Design, Fabrication and Wing Force Control for a Micromechanical Flying Insect*, Ph. D. Dissertation, University of California, Berkeley, Department of Electrical Engineering, Aug 2003.
- [18] A. N. Brooks, P. B. MacCready, P. B. S. Lissaman and W. R. Morgan, Development of a wing-flapping flying replica of the largest pterosaur, *AIAA paper 85-1446* (1985).
- [19] M. B. Bennett, R. F. Ker and R. McN. Alexander, Elastic properties in the tails of cetaceans (*Phocaena* and *Lagenorhynchus*) and their effect on the energy cost of swimming, *Journal of the Zoological Society of London*, 211 (1987) 177-192.
- [20] R. Blickhan and J. Cheng, Energy storage by elastic mechanisms in the tail of large swimmers - a Re-evaluation, *Journal of Theoretical Biology*, Vol. 168, 1994, pp. 315-321.
- [21] C. J. Pennycuik, Elastic energy storage in the primary feather shafts, *Journal of Experimental Biology*, 64 (1976) 677-689.
- [22] T. Weis-Fogh, A rubber-like protein in insect cuticle, *Journal of Experimental Biology*, 37 (1960) 889-907.
- [23] T. Weis-Fogh, Quick estimates of flight fitness in hovering animals, including novel mechanisms for lift production, *Journal of Experimental Biology*, 59 (1973) 169-230.
- [24] H. Fleischer, *Manual of Pneumatic Systems Optimization*, McGraw Hill, Inc. (1995).
- [25] W. L. Green, *Aircraft Hydraulic Systems*, John Wiley and Sons (1985).
- [26] B. C. Abbot, B. Bigland and J. M. Ritchie, The physiological cost of negative work," *Journal of Physiology*, 117 (1952) 380-390.
- [27] V. Giurgiutiu, C. A. Rogers and R. Ruscovici, Power and energy issues in the induced-strain actuation for aerospace adaptive control, *AIAA paper 96-1300* (1996).
- [28] C. O. Johnston, et al., Actuator-work concepts applied to unconventional control devices, *Journal of Aircraft*, 44 (2007) 1459-1468.
- [29] C. O. Johnston, W. H. Mason and C. Han, Unsteady thin airfoil theory revisited for a general deforming airfoil, *Journal of Mechanical Science and Technology*, Under Revision.
- [30] T. Theodorsen, General theory of aerodynamic instability and the mechanism of flutter, NACA Report No. 496 (1935).
- [31] T. Y. Wu, Swimming of a waving plate, *Journal of Fluid Mechanics*, 10 (1961) 321-344.
- [32] W. Shyy, M. Berg and D. Ljungqvist, Flapping and flexible wings for biological and micro air vehicles, *Progress in Aerospace Sciences*, 35 (1999) 455-505.
- [33] J. D. DeLaurier, An aerodynamic model for flapping-wing flight, *Aeronautical Journal*, 97 April (1993) 125-130.
- [34] V. A. Tucker, Bird metabolism during flight, evolution of a theory, *Journal of Experimental Biology*, 58 (1973) 689-709.
- [35] R. T. Jones, The unsteady lift of a wing of finite aspect ratio, NACA Report No. 681 (1940).
- [36] M. I. Woods, J. F. Henderson and G. D. Lock, Energy requirements for the flight of micro air vehicles, *Aeronautical Journal*, 105 (2001) 135-147.
- [37] G. R. Spedding and P. B. S. Lissaman, Technical aspects of microscale flight systems, *Journal of Avian Biology*, 29 (1998) 458-468.
- [38] R. Margaria, *Biomechanics and Energetics of Muscular Exercise*, Clarendon Press, Oxford (1976).



Christopher O. Johnston is currently an Aerospace Engineer in the Aerothermodynamics Branch at NASA Langley Research Center. He received his B.S., M.S., and Ph.D. at Virginia Tech, which is where the present work was performed.



Cheolheui Han received a B.S. degree in Mechanical Engineering from Hanyang University in 1993. He received his M.S. and Ph.D. degrees from Hanyang University in 1998 and 2003, respectively. Then, he worked as a visiting post-doctoral researcher at the Dept. of Aerospace and Ocean Engineering at Virginia Tech, USA.

Dr. Han is currently an Assistant Professor at the Department of Aeronautical and Mechanical Design Engineering.